

# DynRefer: Delving into Region-level Multi-modality Tasks via Dynamic Resolution

Yuzhong Zhao<sup>1\*</sup> Feng Liu<sup>1\*</sup> Yue Liu<sup>1</sup> Mingxiang Liao<sup>1</sup> Chen Gong<sup>2</sup>  
Qixiang Ye<sup>1</sup> Fang Wan<sup>1†</sup>

<sup>1</sup>University of Chinese Academy of Sciences <sup>2</sup>University of Virginia

## Abstract

Region-level multi-modality methods can translate referred image regions to human preferred language descriptions. Unfortunately, most of existing methods using fixed visual inputs remain lacking the resolution adaptability to find out precise language descriptions. In this study, we propose a dynamic resolution approach, referred to as DynRefer, to pursue high-accuracy region-level referring through mimicking the resolution adaptability of human visual cognition. DynRefer first implements stochastic vision-language alignment. It aligns desired language descriptions of multi-modality tasks with images of stochastic resolution, which are constructed by nesting a set of views around the referred region. DynRefer then implements dynamic multi-modality referring, which is realized by selecting views based on image and language priors. This allows the visual information used for referring to better match human preferences, thereby improving the representational adaptability of region-level multi-modality models. Extensive experiments show that DynRefer brings mutual improvement upon tasks including region-level captioning, open-vocabulary region recognition and attribute detection. Last but not least, DynRefer achieves new state-of-the-art on multiple region-level multi-modality tasks using a single model. Code is available at <https://github.com/callsys/DynRefer>.

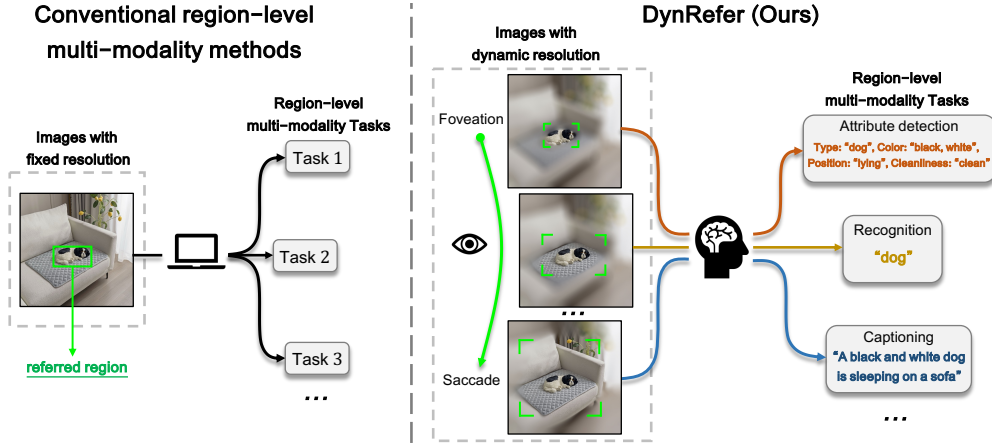


Figure 1: Comparison of the conventional region-level multi-modality methods(left) with DynRefer approach(right). Conventional methods statically encode an image to handle multi-tasks. They lack the resolution adaptability and adequate information encoding. DynRefer follows the mechanism of foveation and saccade in human visual cognition to generate precise language descriptions.

\* Equal contribution. † Corresponding Author.

## 1 Introduction

Region-level multi-modality task, which mimicks the human cognition procedure, is an important branch of artificial intelligence. The objective is to translate the referred image regions into language outputs according to task requirements such as open-vocabulary region recognition [39], attribute detection [4, 8], region-level captioning [59, 37, 7, 17]. Despite of the substantial progress in the past few years, existing methods [24, 51, 4, 8, 69] typically use regions of fixed resolution as inputs, which limits model’s adaptability to region details and the capability of capturing rich context information.

A naive solution is to increase the resolution of the whole input image, to enrich the region representation in both details and image context. Nevertheless, this causes a significant computational cost overhead since popular vision foundation models [13, 14, 23] have already puzzled by the computational complexity, *e.g.*,  $\mathcal{O}(n^2)$  *w.r.t.* the length of input sequence). Besides, it introduces irrelevant region context and thereby posing an additional challenge to the model, which requires to find out the most informative contextual regions.

As is known, the visual cognition system of human is able to adjust the visual input through a process of foveation and saccade eye movements [10, 3] to form non-uniform resolution in response to specific language descriptions, *i.e.*, task requirements. Unfortunately, existing multimodal large language models (MLLMs) [29, 17, 59, 5] remain treating each visual region with equal importance. This results in inadequate encoding of the referred areas and experiences difficulty in capturing visual contextual information matching preferred language expression. This causes the lack of specificity when performing visual feature encoding for specific tasks, which consequently decreases model’s adaptability to multiple tasks.

Motivated by the visual cognition mechanism, *i.e.*, dynamically increasing resolution of the focused area (Foveation) while depressing the irrelevant context (Saccade), we propose the dynamic resolution approach, Fig. 1, towards the following two advantages: (i) *Non-uniformity*. The referred region is of high-resolution, while the irrelevant regions should be of low-resolution or removed. This pushes the models to focus on referred regions for adequate information encoding. (ii) *Adaptability*. The resolution is dynamically adjusted in response to the requirements of language output to customize a resolution for each task. This enhances model’s adaptability to be adaptable to various language output requirements, *i.e.*, multiple multi-modality tasks.

To equip the model with the aforementioned two properties, DynRefer pursues high-accuracy region-level referring by performing stochastic vision-language alignment during training, and dynamic multi-modality referring during inference, Fig. 2. For stochastic vision-language alignment, images with stochastic resolution are first constructed by sampling surrounding views of the referred region. The images are then embedded and aligned to the desired language descriptions of multi-modality tasks. In this way, DynRefer learns the implicit correspondence between dynamic resolutions and specific language descriptions. For dynamic multi-modality referring, proper views are selected to form images with dynamic resolution corresponding to image and language priors.

Extensive experiments conducted on OVAD [4], COCO [32], Visual Genome [25], and RefCOCOG [57] show that DynRefer enjoys high representational capacity and strong task adaptability. With a single model, DynRefer outperforms the state-of-the-art methods about open-vocabulary attribute detection, region recognition, and region-level captioning methods with significant margins. Specifically, DynRefer respectively improves mAP by **1.1%** on OVAD (Open-vocabulary attribute detection), accuracy by **8.8%** on COCO (Open-vocabulary region recognition), mAP by **7.1%** on Visual Genome V1.2 (Dense captioning), and CIDEr by **5.8** on RefCOCOG (Region-level captioning).

The contributions of this study are summarized as follows:

- We propose DynRefer, a simple-yet-effective approach, to pursue high-accuracy region-level referring through mimicking the dynamic resolution mechanism of visual cognition, providing a fresh viewpoint for region-level multi-modality tasks.
- We design a stochastic vision-language alignment procedure, which constructs the implicit correspondence between dynamic resolution inputs and specific language outputs. We further propose a dynamic multi-modality referring procedure, which supports the adaptive prediction of language descriptions for referred regions.

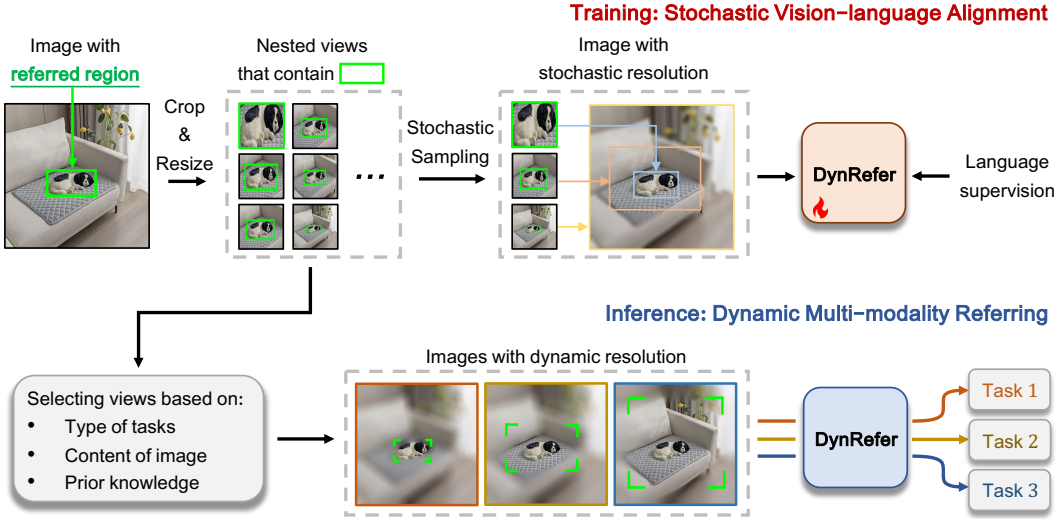


Figure 2: Diagram of the proposed DynRefer. During training, the input image is cropped and resized to multiple views surrounding the referred region. Multiple views are then randomly sampled to simulate a image with stochastic resolution. The sampled views are used to train a DynRefer model (upper). During inference, the views are sampled based on task types, image content, and prior knowledge to meet human preference (lower).

- Extensive experiments on multiple benchmarks show that DynRefer enhances the model’s representational capability and task adaptability. Last but not least, DynRefer achieves the state-of-the-art results for multiple tasks using a single model.

## 2 Related Works

**Vision-Language Models.** These methods aim to learn multi-modality comprehension ability given image-text pairs. Benefiting from powerful foundation models [48, 13, 12, 65, 9] and huge amount of vision-language data corpus [43], VLMs have achieved unprecedented performance across vision-language tasks such as image-text retrieval [28, 29, 50, 31], visual question answering (VQA) [28, 29, 11, 33], image captioning [28, 29, 11, 33], and few-shot learning [1, 56]. According to the training objectives, VLMs can be categorized to three types: (i) Image-text contrastive learning [39, 23, 69, 56, 50], (ii) Image-text matching [27, 28, 29, 2], and (iii) Language modeling [56, 33, 28, 29, 1, 37, 59, 40, 49]. To accomplish region-level tasks, some of these models [37, 59, 40, 4, 69, 49] are trained on region-text pairs to unlock their region-level comprehension ability.

**Region-level Multi-modality Tasks.** The acquirement of preferred semantics (*e.g.*, classes, attributes, captions) for given (referred) image regions is crucial for many multi-modality tasks: (i) Region recognition. With the rapid development of VLMs, classifying regions in an open set has become a common practice. The methods based on contrastive learning [69, 35, 39, 23] get the class by calculating the similarity between region embeddings and text embeddings. While the methods based on language modeling [17, 33, 7, 5, 64] query the large language model (LLM) to select the most likely class of given regions among an open set. (ii) Attribute detection. With the release of large-scale attribute datasets including COCO Attributes [36], Visual Genome [25], and VAW [38], recent studies [38, 60] realize attribute detection by training multi-class classification networks. Inspired by CLIP [39], OVAD [4], OvarNet [8] learn to predict attributes from captions, which rely less on densely annotated attributes and can make predictions in an open vocabulary manner. (iii) Region-level captioning. The generation of region-level captions based on large multimodal models (LMMs) has become a widespread practice [7, 37, 40, 59, 47]. GRiT [51] unifies the training of classification and captioning by treating object categories as brief captions. CapDet [35] further combines dense captioning with open-world detection in a pretraining setup.

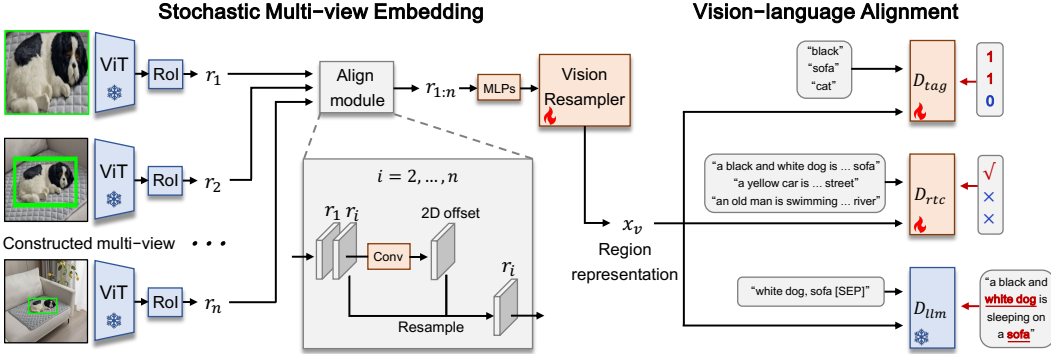


Figure 3: Architecture of the proposed DynRefer. It comprises a stochastic multi-view embedding module and multi-modality decoders ( $D_*$ ).  $n$  nested views are encoded as the region representation  $x_v$  by the stochastic multi-view embedding module (left). The region representation  $x_v$  is decoded by multi-modality decoders, and then aligned to language descriptions of multi-modality tasks (right).

The trend of exploiting region-level information for fine-grained vision-language tasks urges the development of resolution adaptability, which is crucial to improve the accuracy of recognition, attribute detection, and region-level captioning by dynamically using the context information. Furthermore, for the multiple types of referring tasks, existing methods ignore the inherent similarity between region-level multi-modality tasks. There is an urgent requirement to unify these tasks from the perspective of model training. Such unification is expected to bring mutual improvement among tasks so that state-of-the-art results can be achieved for all tasks with a single model.

**Dynamic Resolution of Visual Cognition.** The research in the visual cognition area has shown that the human vision system has the capability of dynamic resolution. The fovea, situated in the central part of the retina, possesses the highest resolution view, while other parts of the retina dynamically perceive context views for details [10]. Recent research [3] has demonstrated that foveal and peripheral vision are closely linked and differences in appearance between peripheral and foveal vision can be adjusted through re-calibration [46]. In contrast, computer vision systems lack such a dynamic mechanism and instead capture only a static view [18]. To simulate the dynamic resolution mechanism through computer vision is non-trivial.

Please refer to Appendix A for a more comprehensive discussion of related works.

### 3 Methodology

DynRefer consists of a stochastic vision-language alignment procedure and a dynamic multi-modality referring procedure, Fig. 2. In the stochastic vision-language alignment procedure, we construct multiple views of the input image to simulate stochastic resolution. A stochastic multi-view embedding procedure is then carried out to encode the image regions under stochastic resolution to region representation, which is aligned to language descriptions of multi-modality tasks. In the dynamic multi-modality referring procedure, multiple views are constructed once again, and proper views are optimally selected to match human preferences, thereby improving the representational adaptability of region-level multi-modality models.

#### 3.1 Stochastic Vision-Language Alignment

##### 3.1.1 Multi-view Construction

Vision foundation models, *e.g.*, CLIP and EVA-CLIP [23, 14], are becoming more powerful, but remain handling fixed-resolution images. To exploit their potential for encoding visual inputs of dynamic resolution, we seek a simple alternative by transforming the original image into multiple nested views that cover the referred regions. These nested views share the same resolution and can be combined to simulate an image with dynamic resolution, highlighting the referred region while depressing the irrelevant areas, Fig. 2(upper).

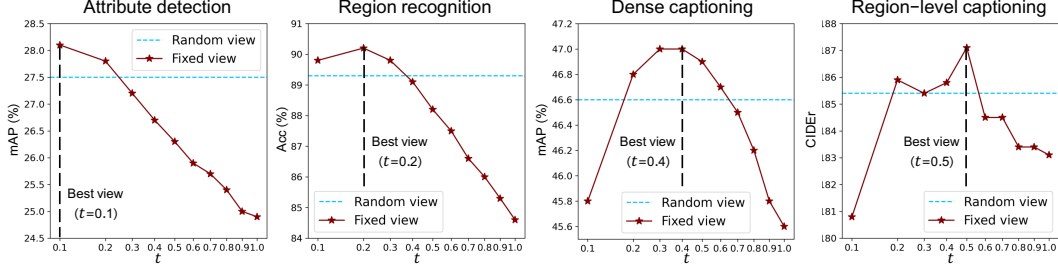


Figure 4: Performance of a double-view ( $n = 2$ ) DynRefer model on region-level multi-modality tasks (e.g., open-vocabulary attribute detection on OVAD [4], region recognition on COCO [32], dense captioning on VG-COCO [44], and region-level captioning on VG [25]) under different interpolation coefficients  $\mathbf{t}$ ,  $\mathbf{t} = [t_1, t_2] \in \mathbb{R}^2[0, 1]$ . The first view is a fixed one ( $t_1 = 0$ ) and the second is randomly selected or fixed.

In specific, the original image  $x$  is cropped and resized into multiple candidate views. The cropped regions are calculated by  $b_r + t * (b_x - b_r)$ ,  $t \in \mathbb{R}[0, 1]$ .  $b_r$ ,  $b_x$ , and  $t$  respectively denote the bounding box of the referred region, the size of the whole image, and the interpolation coefficient. During training,  $n$  views are stochastic sampled from the candidates to simulate images generated by foveation and saccadic eye movements. The  $n$  views correspond to interpolation coefficients  $\mathbf{t}, \mathbf{t} = [t_1, t_2, \dots, t_n]$ . We keep the view containing only the referred region ( $t_1 = 0$ ) being sampled, which best preserves details and is experimentally validated crucial for all multi-modality tasks.

### 3.1.2 Stochastic Multi-view Embedding

The sampled  $n$  views, *i.e.*, image regions under stochastic resolution, are jointly encoded by a frozen ViT into spatial features, which are further processed by an ROI-Align module [19] to obtain region embeddings, *i.e.*,  $\{r_i\}_{i=1,2,\dots,n}$ , Fig. 3(left).

Due to biases introduced by cropping, resizing, and ROI-Align, the region embeddings are not well spatially aligned. Inspired by dynamic convolution operations [53, 21], we propose an align module to reduce the bias by aligning  $\{r_i\}_{i=2,3,\dots,n}$  to  $r_1$ , where  $r_1$  is the region embedding corresponds to the view containing only the referred region. For each region embedding  $r_i$ , it is first concatenated with  $r_1$ , followed by a convolution layer to compute a 2D offset map. The spatial feature of  $r_i$  is then resampled according to the 2D offset. Finally, the aligned region embeddings are concatenated across the channel dimension and fused by a multi-layer perceptron (MLP) layer. The outputs are further compressed by a vision resampling module, *i.e.*, the Q-former [29], so that we extract a region representation ( $x_v$  in Fig. 3) for the referred region  $b_r$  of the original image  $x$ .

### 3.1.3 Vision-Language Alignment

The region representation  $x_v$ , calculated through a stochastic multi-view embedding module, is decoded by three decoders<sup>2</sup>.  $D_*$  is shown in Fig. 3(right), which are respectively supervised by three multi-modality tasks:

**i) Image Region Tagging.** Inspired by the off-the-shelf image tagging methods [34, 22, 66], we apply a query-based lightweight recognition decoder [34] for region tagging. The decoder  $D_{tag}$  is shown in Fig. 3(right). This tagging procedure is fulfilled through calculating the confidence of predefined tags by using tags as query and  $x_v$  as key and value, respectively. Following the control captioning method [68], we parse the ground-truth tags from the captions to supervise the recognition decoder. To handle the problem of missing labels of regions, the asymmetric loss [41], which is robust to imprecise supervision, is used for model optimization.

**ii) Region-text Contrastive Learning.** Similar to the decoder for region tagging, the decoder  $D_{rtc}$  is defined as a query-based recognition decoder [34], which calculates the similarity scores between captions and region features by using the former as the query and the latter as the key and value. This actually is a contrastive learning procedure, where the similarity scores are optimized through the

<sup>2</sup>Please refer to Appendix C for more details about the decoders.

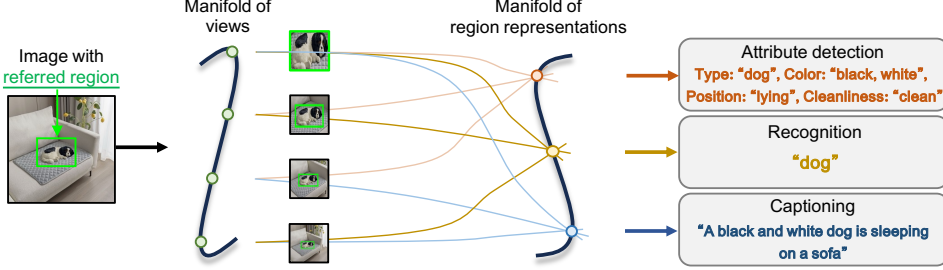


Figure 5: Understanding DynRefer from a perspective of manifold.

pairwise Sigmoid loss for Language-Image Pre-training [62]. Unlike standard contrastive learning with softmax normalization, the sigmoid loss operates solely on image-text pairs and does not require a global view of the pairwise similarities for normalization.

**iii) Language Modeling.** As shown in Fig. 3(right), a language modeling decoder  $D_{llm}$  is used to convert region representation  $x_v$  to language descriptions. Following the typical design of LLMs [29, 33], a learnable linear projector is used to map  $x_v$  to the language space. Together with the mapped  $x_v$ , random control embeddings<sup>3</sup> [68] built upon word pieces parsed from the ground-truth captions are fed to a frozen LLM for text generation. The language outputs are supervised by the ground-truth captions with a cross-entropy loss [68, 29, 33].

### 3.2 Dynamic Multi-Modality Referring

During the inference procedure, the trained DynRefer model performs multi-modality referring on images through dynamic resolution. By adjusting the interpolation coefficients  $\mathbf{t}(\mathbf{t} = [t_1, t_2, \dots, t_n])$  of sampled  $n$  views, it results in region representations of dynamic resolution characteristics. This is consistent with the training procedure.

To evaluate the effect of the dynamic resolution characteristics, we train a double-view ( $n = 2$ ) DynRefer model and evaluate it on three multi-modality tasks. From the curves in Fig. 4, we can conclude that better results are achieved for attribute detection under context-less views ( $t_2 = 0.1$ ), which refer to an image region tightly bound to the referred region. This is explainable as such a task typically requires region details. Region-level captioning and dense captioning require context-rich views ( $t_2 = 0.4$  or  $t_2 = 0.5$ ) as it prefers rich context for a complete understanding of the referred region. It is worth noting that views of too much context ( $t_2 > 0.5$ ) deteriorates the performance of all tasks as they introduce excessively region-irrelevant information.

When task priors are known, one can sample the appropriate views according to the characteristics of the tasks. When task priors are agnostic, it requires to first construct a set of candidate views under different interpolation coefficients  $t$ ,  $t \in \{0.1, 0.2, \dots, 1\}$ . From the candidates,  $n$  views are sampled through a greedy search algorithm. The search objective function is formulated as

$$\operatorname{argmax}_{t_i} \sum (\text{pHASH}(x(t_1)) \oplus \text{pHASH}(x(t_i))) / t_i, t_i \in \mathbb{R}[0, 1] \quad (1)$$

where  $t_i$ ,  $x(t_i)$ ,  $\text{pHASH}(\cdot)$  and  $\oplus$  respectively denotes the interpolation coefficient of the  $i$ -th view, the  $i$ -th view, the perceptual image hash function and XOR operation. To compare the information of views from a global perspective, we leverage the “pHASH(·)” function to transform views from the spatial domain to the frequency domain and then encode them into hash codes. For the term “ $\oplus$ ”, we aim to find an informative view that has incremental information compared to the view containing only the referred region. For the term “ $1/t_i$ ”, we attenuate the weight of context-rich views to avoid introducing too much redundant information.

### 3.3 Discussion: A Manifold Perspective

Conventional resolution-fixed methods [37, 59, 17] have been challenged by diverse multi-modality tasks, as the fixed region representation  $x_v$  is not powerful enough to support these tasks at the same time. In contrast, DynRefer learns a manifold of region representation  $x_v(\mathbf{t})$ , Fig. 5. On the manifold,

<sup>3</sup>More details of the control embeddings are provided in Appendix C.

Table 1: Region-level captioning performance of the proposed approach and the state-of-the-art methods on the RefCOCOg and VG datasets.

Method	Model size	RefCOCOg		VG	
		METEOR	CIDEr	METEOR	CIDEr
SLR+Rerank <sub>CVPR'17</sub> [58]	<1B	15.9	66.2	-	-
GRiT <sub>ARXIV'22</sub> [51]	<1B	15.2	71.6	17.1	142.0
Kosmos-2 <sub>ICLR'24</sub> [37]	1.6B	14.1	62.3	-	-
GPT4RoI <sub>ARXIV'23</sub> [64]	7B	-	-	17.4	145.2
RegionGPT <sub>CVPR'24</sub> [40]	7B	16.9	109.9	17.0	145.6
GLaMM <sub>CVPR'24</sub> [40]	7B	16.2	105.0	18.6	157.8
Alpha-CLIP+LLaVA <sub>CVPR'24</sub> [47]	7B	16.7	109.2	18.9	160.3
Osprey <sub>CVPR'24</sub> [59]	7B	16.6	108.3	-	-
DynRefer (Ours)	4.2B	<b>18.1</b>	<b>115.7</b>	<b>21.2</b>	<b>190.9</b>

Table 2: Dense captioning performance of the proposed approach and the state-of-the-art methods on the VG and VG-COCO datasets.

Methods	GT localization	mAP(%)		
		VG V1.0	VG V1.2	VG-COCO
GRiT <sub>ARXIV'22</sub> [51]	✗	15.5	16.4	-
CapDet <sub>CVPR'23</sub> [35]	✗	-	15.4	14.0
DCMSTRD <sub>TMM'24</sub> [45]	✗	13.6	13.4	16.1
DynRefer (Ours)	✗	<b>19.1</b>	<b>19.5</b>	<b>19.4</b>
GRiT <sub>ARXIV'22</sub> [51]	✓	40.0	40.3	-
BLIP2 <sub>ICML'23</sub> [29]	✓	37.7	37.9	36.9
DynRefer (Ours)	✓	<b>47.2</b>	<b>47.4</b>	<b>47.6</b>

weaker yet more dense representation can be sampled by adjusting the interpolation coefficients  $\mathbf{t}$  of views. Such dense representation facilitates precise matching with the language embeddings, which consequently brings large performance gains for multi-modality tasks. More discussion of the manifold perspective is provided in Appendix B.

## 4 Experiment

DynRefer is implemented upon the LAVIS [26] framework, where large language model and vision resampler are respectively initialized by Flan-T5<sub>XL</sub> [9] and Q-former [29]. All the sampled views are resized to  $224 \times 224$  resolution. All models can be trained less than 20 hours using 8 NVIDIA A800 GPUs. For performance comparison, DynRefer is trained on VG V1.2 [25] (*i.e.*, results in Tab. 1 2 3 4). For ablation studies, DynRefer is trained on VG-COCO [44] (*i.e.*, results in Tab. 5). For results on RefCOCOg [57], DynRefer is finetuned on its training set. Please refer to Appendix E for more details about model/dataset/evaluation settings.

### 4.1 Performance

**Region-level Captioning.** In Tab. 1 and Tab. 2, DynRefer is compared with the state-of-the-art (SOTA) methods. DynRefer respectively achieves 18.1 and 21.2 METEOR scores, 115.7 and 190.9 CIDEr scores on RefCOCOg and VG, outperforming the SOTA methods with a much smaller model size (4.2B *vs.* 7B). For dense captioning, DynRefer respectively achieves 19.1%, 19.5% and 19.4% mAPs on VG V1.0, V1.2, and VG-COCO, outperforming the SOTA methods by significant margins. When ground-truth bounding boxes are given, DynRefer respectively achieves 47.2%, 47.4% and 47.6% mAPs on VG V1.0, V1.2, and VG-COCO, outperforming GRiT [51] by 7.1% on VG1.2.

**Open-Vocabulary Attribute Detection.** The performance is shown in Tab. 3. DynRefer achieves 29.2% mAP on OVAD, outperforming the SOTA methods. On Medium and Tail attributes, DynRefer achieves the highest mAP, which demonstrates the generalizability of the proposed approach.

Table 3: Open vocabulary attribute detection performance of the proposed approach and the state-of-the-art methods on the OVAD dataset with the box-oracle setup (OVAD-Box).

Method	Backbone	OVAD-Box			
		All	Head	Medium	Tail
CLIP <sub>ICML'21</sub> [39]	ViT-B16	16.6	43.9	18.6	4.4
ALBEF <sub>NeurIPS'21</sub> [27]	ViT-B16	21.0	44.2	23.9	9.4
X-VLM <sub>ICML'22</sub> [61]	Swin-B	28.1	49.7	34.2	12.9
OVAD-Baseline-Box <sub>CVPR'23</sub> [4]	ViT-B32	21.4	48.0	26.9	5.2
BLIP2 <sub>ICML'23</sub> [29]	EVA	25.5	49.8	30.5	10.8
DynRefer (Ours)	ViT-L	28.2	50.9	34.5	12.5
DynRefer (Ours)	EVA	<b>29.2</b>	49.9	<b>35.7</b>	<b>14.0</b>

Table 4: Open vocabulary region recognition performance of the proposed approach and state-of-the-art methods on the COCO-2017 val set. Following RegionGPT [17] and RegionCLIP [69], we report the results of object classification given ground-truth boxes.

Method	Backbone	LLM	mAP	Acc. (%)
CLIP <sub>ICML'21</sub> [39]	ViT-L	-	58.9	-
RegionCLIP <sub>CVPR'22</sub> [69]	R50	-	58.3	-
LLaVA <sub>NeurIPS'23</sub> [33]	ViT-L	Vicuna-7B	-	40.0
Shikra <sub>ARXIV'23</sub> [7]	ViT-L	Vicuna-7B	-	53.9
GPT4RoI <sub>ARXIV'23</sub> [64]	ViT-L	LLaVA-7B	-	64.0
PVIT <sub>ARXIV'23</sub> [5]	ViT-L+R50	LLaVA-7B	-	64.5
ASM <sub>ICLR'24</sub> [49]	ViT-L	Hasky-7B	69.3	-
RegionGPT <sub>CVPR'24</sub> [17]	ViT-L	Vicuna-7B	70.0	80.6
DynRefer (Ours)	ViT-L	FlanT5 <sub>XL</sub> -3.4B	85.0	89.4
DynRefer (Ours)	EVA	FlanT5 <sub>XL</sub> -3.4B	<b>89.2</b>	<b>91.8</b>

**Open-Vocabulary Region Recognition.** The performance is shown in Tab. 4. DynRefer outperforms the SOTA methods by large margins (up to 8.8% Acc. and 15% mAP) with a smaller language model.

**Multi-task Capability.** Fig. 6 shows DynRefer ‘s capability for multi-task multi-modality referring, *i.e.*, generating region-level captions, tags, attributes, and classes using a single model.

## 4.2 Ablation Studies

**Stochastic Multi-view Embedding.** In Tab. 5, we compare the proposed stochastic multi-view embedding approach with other commonly used region representation methods [29, 64, 68]. In lines 1-2, the model is trained with resolution-fixed images. In lines 3-4, we increase the resolution of the input images based on line 2 following common practice [59], which brings higher FLOPs and limited performance gain. In line 5, the model is trained with visual input of fixed 2-view, which has acceptable FLOPs and large performance gain, demonstrating the efficiency of encoding images of dynamic resolution. In lines 6-8, the views are stochastically sampled during training, which brings performance gain on all tasks with no extra cost, demonstrating the effectiveness of simulating the mechanism of foveation and saccade in human cognition. In lines 9-10, we increase the number of sampled views, which further improves the performance at an acceptable cost of FLOPs.

**Vision-Language Alignment.** The effectiveness of aligning region representations of images to language descriptions of multi-tasks is validated in lines 10-13, Tab. 5. Dropping any decoder will degrade performance, demonstrating the mutual improvements among tasks.

**Dynamic Multi-modality Referring.** The effectiveness of selecting views dynamically is evaluated in lines 6-10 in Tab. 5. Compared to randomly selected views during inference, the proposed selection strategy effectively improves the performance on all tasks in a task-agnostic manner.

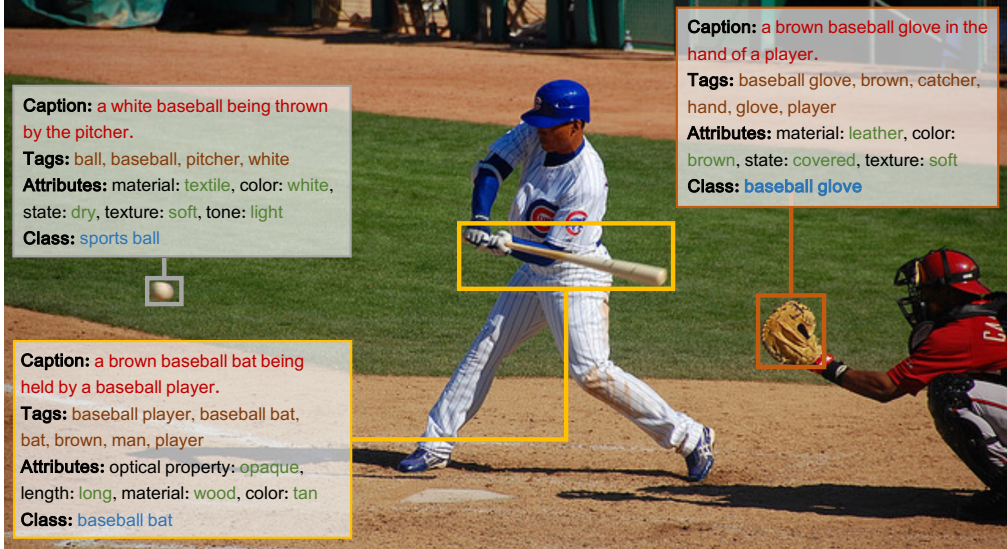


Figure 6: Illustration of DynRefer’s multi-task capability. It can generate captions (red), tags (brown), attributes (green), classes (blue), using a single model, for multiple referred regions.

Table 5: Ablation studies of DynRefer on region-level multi-modality benchmarks. Line 1: Training with cropped images [29]. Line 2: Training with images with ROI-Align [64, 40]. Lines 3-4: Training with higher resolution images. Line 5: Training with fixed 2-view [68]. Lines 6-10: Training with stochastic  $n$ -view (Ours). Lines 11-13: Based on line 10, removing decoders  $D_*$  in Sec. 3.1.3. For model inference, “random”, “dynamic”, “best” respectively denotes inference with randomly selected views, selection strategy proposed in Sec. 3.2, and the best views(*i.e.*, manually selected based on the result of the test set). “V. FLOPs” denotes the FLOPs of the vision encoder, *e.g.*, ViT, align module, vision resampler in Fig. 3. More details of the ablation studies are provided in Appendix E

	Training	Inference	V. FLOPs	OVAD mAP (%)	COCO Acc. (%)	VG-COCO mAP (%)	RefCOCOg	
							CIDEr	METEOR
1	cropped image	-	268G	23.0	77.0	40.0	107.3	17.1
2	image + ROIAlign	-	268G	19.7	74.3	39.1	110.0	17.2
3	+ reso. 224 $\rightarrow$ 336	-	618G	21.7	80.1	41.5	111.3	17.4
4	+ reso. 224 $\rightarrow$ 448	-	1146G	22.7	81.2	41.8	113.0	17.3
5	fixed 2-view	-	530G	25.4	85.4	45.8	114.2	17.9
6	stochastic 2-view	random	530G	26.1	87.8	46.6	114.4	17.9
7	stochastic 2-view	dynamic	530G	27.5	89.3	46.8	114.7	17.9
8	stochastic 2-view	best	530G	28.1	90.2	47.0	115.6	18.1
9	stochastic 3-view	random	792G	27.3	88.9	47.3	117.7	18.2
10	stochastic 3-view	dynamic	792G	<b>28.7</b>	<b>90.3</b>	<b>47.4</b>	<b>118.6</b>	<b>18.2</b>
11	- $D_{lm}$	dynamic	792G	27.6	89.0	-	-	-
12	- $D_{rc}$	dynamic	792G	-	-	47.0	114.2	18.1
13	- $D_{tag}$	dynamic	792G	27.0	90.3	44.8	118.4	16.7

## 5 Conclusion

We present DynRefer, a resolution-adaptive approach to pursue high-accuracy region-level referring through mimicking the resolution adaptability of human visual cognition. With stochastic vision-language alignment and dynamic multi-modality referring, DynRefer predicts desired language descriptions for multi-modality tasks, as well as customizing the resolution of referred image regions according to the image and language priors. With its powerful adaptability, DynRefer improves the performance of region-level multi-modality tasks, with striking contrast to the state-of-the-art methods. DynRefer provides a fresh insight to unify region-level multi-modality tasks.

## References

- [1] Jean-Baptiste Alayrac, Jeff Donahue, Pauline Luc, Antoine Miech, Iain Barr, Yana Hasson, Karel Lenc, Arthur Mensch, Katherine Millican, Malcolm Reynolds, Roman Ring, Eliza Rutherford, Serkan Cabi, Tengda Han, Zhitao Gong, Sina Samangooei, Marianne Monteiro, Jacob L. Menick, Sebastian Borgeaud, Andy Brock, Aida Nematzadeh, Sahand Sharifzadeh, Mikolaj Binkowski, Ricardo Barreira, Oriol Vinyals, Andrew Zisserman, and Karén Simonyan. Flamingo: a visual language model for few-shot learning. In *NeurIPS*, 2022.
- [2] Hangbo Bao, Wenhui Wang, Li Dong, Qiang Liu, Owais Khan Mohammed, Kriti Aggarwal, Subhrojit Som, Songhao Piao, and Furu Wei. Vlmo: Unified vision-language pre-training with mixture-of-modality-experts. *NeurIPS*, 35:32897–32912, 2022.
- [3] P. Binda and M. C. Morrone. Vision during saccadic eye movements. *The Journal of Comparative Neurology*, 292(4):497–523,, 1990.
- [4] Maria A Bravo, Sudhanshu Mittal, Simon Ging, and Thomas Brox. Open-vocabulary attribute detection. In *IEEE CVPR*, pages 7041–7050, 2023.
- [5] Chi Chen, Ruoyu Qin, Fuwen Luo, Xiaoyue Mi, Peng Li, Maosong Sun, and Yang Liu. Position-enhanced visual instruction tuning for multimodal large language models. *arXiv preprint arXiv:2308.13437*, 2023.
- [6] Jun Chen, Deyao Zhu, Xiaoqian Shen, Xiang Li, Zechun Liu, Pengchuan Zhang, Raghuraman Krishnamoorthi, Vikas Chandra, Yunyang Xiong, and Mohamed Elhoseiny. Minigpt-v2: large language model as a unified interface for vision-language multi-task learning. *arXiv preprint arXiv:2310.09478*, 2023.
- [7] Keqin Chen, Zhao Zhang, Weili Zeng, Richong Zhang, Feng Zhu, and Rui Zhao. Shikra: Unleashing multimodal llm’s referential dialogue magic. *arXiv preprint arXiv:2306.15195*, 2023.
- [8] Keyan Chen, Xiaolong Jiang, Yao Hu, Xu Tang, Yan Gao, Jianqi Chen, and Weidi Xie. Ovarnet: Towards open-vocabulary object attribute recognition. In *IEEE CVPR*, pages 23518–23527, 2023.
- [9] Hyung Won Chung, Le Hou, Shayne Longpre, Barret Zoph, Yi Tay, William Fedus, Eric Li, Xuezhi Wang, Mostafa Dehghani, Siddhartha Brahma, Albert Webson, Shixiang Shane Gu, Zhuyun Dai, Mirac Suzgun, Xinyun Chen, Aakanksha Chowdhery, Sharan Narang, Gaurav Mishra, Adams Yu, Vincent Y. Zhao, Yanping Huang, Andrew M. Dai, Hongkun Yu, Slav Petrov, Ed H. Chi, Jeff Dean, Jacob Devlin, Adam Roberts, Denny Zhou, Quoc V. Le, and Jason Wei. Scaling instruction-finetuned language models. *arXiv preprint arXiv:2210.11416*, 2022.
- [10] C. A. Curcio, Sloan K. R., Kalina R. E., and A. E. Hendrickson. Human photoreceptor topography. *The Journal of Comparative Neurology*, 292(4):497–523,, 1990.
- [11] Wenliang Dai, Junnan Li, Dongxu Li, Anthony Meng Huat Tiong, Junqi Zhao, Weisheng Wang, Boyang Li, Pascale Fung, and Steven C. H. Hoi. Instructblip: Towards general-purpose vision-language models with instruction tuning. *arXiv preprint arXiv:2305.06500*, 2023.
- [12] Jacob Devlin, Ming-Wei Chang, Kenton Lee, and Kristina Toutanova. BERT: pre-training of deep bidirectional transformers for language understanding. In Jill Burstein, Christy Doran, and Thamar Solorio, editors, *NAACL*, pages 4171–4186, 2019.
- [13] Alexey Dosovitskiy, Lucas Beyer, Alexander Kolesnikov, Dirk Weissenborn, Xiaohua Zhai, Thomas Unterthiner, Mostafa Dehghani, Matthias Minderer, Georg Heigold, Sylvain Gelly, Jakob Uszkoreit, and Neil Houlsby. An image is worth 16x16 words: Transformers for image recognition at scale. In *ICLR*, 2021.
- [14] Yuxin Fang, Wen Wang, Binhui Xie, Quan Sun, Ledell Wu, Xinggang Wang, Tiejun Huang, Xinlong Wang, and Yue Cao. Eva: Exploring the limits of masked visual representation learning at scale. In *IEEE CVPR*, pages 19358–19369, 2023.
- [15] Ali Farhadi, Ian Endres, Derek Hoiem, and David Forsyth. Describing objects by their attributes. In *IEEE CVPR*, pages 1778–1785, 2009.
- [16] Ross Girshick. Fast r-cnn. In *IEEE ICCV*, pages 1440–1448, 2015.
- [17] Qiushan Guo, Shalini De Mello, Hongxu Yin, Wonmin Byeon, Ka Chun Cheung, Yizhou Yu, Ping Luo, and Sifei Liu. Regionpt: Towards region understanding vision language model, 2024.
- [18] Strasburger H. even myths on crowding and peripheral vision. *i-Perception*, 11(3):1–46, 2018.
- [19] Kaiming He, Georgia Gkioxari, Piotr Dollár, and Ross Girshick. Mask r-cnn. In *IEEE ICCV*, pages 2961–2969, 2017.
- [20] Chen Huang, Yining Li, Chen Change Loy, and Xiaoou Tang. Deep imbalanced learning for face recognition and attribute prediction. *IEEE TPAMI*, 42(11):2781–2794, 2019.
- [21] Shihua Huang, Zhichao Lu, Ran Cheng, and Cheng He. Fapn: Feature-aligned pyramid network for dense image prediction. In *Proceedings of the IEEE/CVF international conference on computer vision*, pages 864–873, 2021.

- [22] Xinyu Huang, Youcai Zhang, Jinyu Ma, Weiwei Tian, Rui Feng, Yuejie Zhang, Yaqian Li, Yandong Guo, and Lei Zhang. Tag2text: Guiding vision-language model via image tagging. *arXiv preprint arXiv:2303.05657*, 2023.
- [23] Gabriel Ilharco, Mitchell Wortsman, Ross Wightman, Cade Gordon, Nicholas Carlini, Rohan Taori, Achal Dave, Vaishaal Shankar, Hongseok Namkoong, John Miller, Hannaneh Hajishirzi, Ali Farhadi, and Ludwig Schmidt. Openclip, July 2021. URL <https://doi.org/10.5281/zenodo.5143773>. If you use this software, please cite it as below.
- [24] Justin Johnson, Andrej Karpathy, and Li Fei-Fei. Densecap: Fully convolutional localization networks for dense captioning. In *IEEE CVPR*, pages 4565–4574, 2016.
- [25] Ranjay Krishna, Yuke Zhu, Oliver Groth, Justin Johnson, Kenji Hata, Joshua Kravitz, Stephanie Chen, Yannis Kalantidis, Li-Jia Li, David A Shamma, et al. Visual genome: Connecting language and vision using crowdsourced dense image annotations. *IJCV*, pages 32–73, 2017.
- [26] Dongxu Li, Junnan Li, Hung Le, Guangsen Wang, Silvio Savarese, and Steven CH Hoi. Lavis: A library for language-vision intelligence. *arXiv preprint arXiv:2209.09019*, 2022.
- [27] Junnan Li, Ramprasaath Selvaraju, Akhilesh Gotmare, Shafiq Joty, Caiming Xiong, and Steven Chu Hong Hoi. Align before fuse: Vision and language representation learning with momentum distillation. *NeurIPS*, 34:9694–9705, 2021.
- [28] Junnan Li, Dongxu Li, Caiming Xiong, and Steven C. H. Hoi. BLIP: bootstrapping language-image pre-training for unified vision-language understanding and generation. In *ICML*, pages 12888–12900, 2022.
- [29] Junnan Li, Dongxu Li, Silvio Savarese, and Steven C. H. Hoi. BLIP-2: bootstrapping language-image pre-training with frozen image encoders and large language models. In *ICML*, pages 19730–19742, 2023.
- [30] Xiangyang Li, Shuqiang Jiang, and Jungong Han. Learning object context for dense captioning. In *AAAI*, pages 8650–8657, 2019.
- [31] Xiujun Li, Xi Yin, Chunyuan Li, Pengchuan Zhang, Xiaowei Hu, Lei Zhang, Lijuan Wang, Houdong Hu, Li Dong, Furu Wei, et al. Oscar: Object-semantics aligned pre-training for vision-language tasks. In *ECCV*, pages 121–137, 2020.
- [32] Tsung-Yi Lin, Michael Maire, Serge Belongie, James Hays, Pietro Perona, Deva Ramanan, Piotr Dollár, and C Lawrence Zitnick. Microsoft coco: Common objects in context. In *ECCV*, pages 740–755, 2014.
- [33] Haotian Liu, Chunyuan Li, Qingyang Wu, and Yong Jae Lee. Visual instruction tuning. *NeurIPS*, 36, 2023.
- [34] Shilong Liu, Lei Zhang, Xiao Yang, Hang Su, and Jun Zhu. Query2label: A simple transformer way to multi-label classification. *arXiv preprint arXiv:2107.10834*, 2021.
- [35] Yanxin Long, Youpeng Wen, Jianhua Han, Hang Xu, Pengzhen Ren, Wei Zhang, Shen Zhao, and Xiaodan Liang. Capdet: Unifying dense captioning and open-world detection pretraining. In *IEEE CVPR*, pages 15233–15243, 2023.
- [36] Genevieve Patterson and James Hays. Coco attributes: Attributes for people, animals, and objects. In *ECCV*, pages 85–100, 2016.
- [37] Zhiliang Peng, Wenhui Wang, Li Dong, Yaru Hao, Shaohan Huang, Shuming Ma, and Furu Wei. Kosmos-2: Grounding multimodal large language models to the world. *ICLR*, 2024.
- [38] Khoi Pham, Kushal Kafle, Zhe Lin, Zhihong Ding, Scott Cohen, Quan Tran, and Abhinav Shrivastava. Learning to predict visual attributes in the wild. In *IEEE CVPR*, pages 13018–13028, 2021.
- [39] Alec Radford, Jong Wook Kim, Chris Hallacy, Aditya Ramesh, Gabriel Goh, Sandhini Agarwal, Girish Sastry, Amanda Askell, Pamela Mishkin, Jack Clark, Gretchen Krueger, and Ilya Sutskever. Learning transferable visual models from natural language supervision. In *ICML*, pages 8748–8763, 2021.
- [40] Hanoona Rasheed, Muhammad Maaz, Sahal Shaji, Abdelrahman Shaker, Salman Khan, Hisham Cholakkal, Rao M. Anwer, Eric Xing, Ming-Hsuan Yang, and Fahad S. Khan. Glamm: Pixel grounding large multimodal model. *IEEE CVPR*, 2024.
- [41] Tal Ridnik, Emanuel Ben-Baruch, Nadav Zamir, Asaf Noy, Itamar Friedman, Matan Protter, and Lih Zelnik-Manor. Asymmetric loss for multi-label classification. In *IEEE CVPR*, pages 82–91, 2021.
- [42] Robin Rombach, Andreas Blattmann, Dominik Lorenz, Patrick Esser, and Björn Ommer. High-resolution image synthesis with latent diffusion models. In *IEEE CVPR*, pages 10674–10685, 2022.
- [43] Christoph Schuhmann, Romain Beaumont, Richard Vencu, Cade Gordon, Ross Wightman, Mehdi Cherti, Theo Coombes, Aarush Katta, Clayton Mullis, Mitchell Wortsman, et al. Laion-5b: An open large-scale dataset for training next generation image-text models. *NeurIPS*, pages 25278–25294, 2022.
- [44] Zhuang Shao, Jungong Han, Demetris Marnerides, and Kurt Debattista. Region-object relation-aware dense captioning via transformer. *IEEE TNNLS*, 2022.

- [45] Zhuang Shao, Jungong Han, Kurt Debattista, and Yanwei Pang. Dcmstrd: End-to-end dense captioning via multi-scale transformer decoding. *IEEE Transactions on Multimedia*, pages 1–13, 2024. doi: 10.1109/TMM.2024.3369863.
- [46] E. E. M. Stewart and Schütz A. C. Attention modulates trans-saccadic integration. *The Journal of Comparative Neurology*, 142:1–10, 2018.
- [47] Zeyi Sun, Ye Fang, Tong Wu, Pan Zhang, Yuhang Zang, Shu Kong, Yuanjun Xiong, Dahua Lin, and Jiaqi Wang. Alpha-clip: A clip model focusing on wherever you want. *IEEE CVPR*, 2024.
- [48] Ashish Vaswani, Noam Shazeer, Niki Parmar, Jakob Uszkoreit, Llion Jones, Aidan N Gomez, Łukasz Kaiser, and Illia Polosukhin. Attention is all you need. *NeurIPS*, 2017.
- [49] Weiyun Wang, Min Shi, Qingyun Li, Wenhai Wang, Zhenhang Huang, Linjie Xing, Zhe Chen, Hao Li, Xizhou Zhu, Zhiguo Cao, et al. The all-seeing project: Towards panoptic visual recognition and understanding of the open world. *ICLR*, 2024.
- [50] Wenhui Wang, Hangbo Bao, Li Dong, Johan Bjorck, Zhiliang Peng, Qiang Liu, Kriti Aggarwal, Owais Khan Mohammed, Saksham Singhal, Subhajit Som, and Furu Wei. Image as a foreign language: Beit pretraining for all vision and vision-language tasks. *arXiv preprint arXiv:2208.10442*, 2022.
- [51] Jialian Wu, Jianfeng Wang, Zhengyuan Yang, Zhe Gan, Zicheng Liu, Junsong Yuan, and Lijuan Wang. Grit: A generative region-to-text transformer for object understanding. *arXiv preprint arXiv:2212.00280*, 2022.
- [52] Yongqin Xian, Bernt Schiele, and Zeynep Akata. Zero-shot learning—the good, the bad and the ugly. In *IEEE CVPR*, pages 4582–4591, 2017.
- [53] Yuwen Xiong, Zhiqi Li, Yuntao Chen, Feng Wang, Xizhou Zhu, Jiapeng Luo, Wenhai Wang, Tong Lu, Hongsheng Li, Yu Qiao, Lewei Lu, Jie Zhou, and Jifeng Dai. Efficient deformable convnets: Rethinking dynamic and sparse operator for vision applications. *arXiv preprint arXiv:2401.06197*, 2024.
- [54] Linjie Yang, Kevin Tang, Jianchao Yang, and Li-Jia Li. Dense captioning with joint inference and visual context. In *IEEE CVPR*, pages 2193–2202, 2017.
- [55] Guojun Yin, Lu Sheng, Bin Liu, Nenghai Yu, Xiaogang Wang, and Jing Shao. Context and attribute grounded dense captioning. In *IEEE CVPR*, pages 6241–6250, 2019.
- [56] Jiahui Yu, Zirui Wang, Vijay Vasudevan, Legg Yeung, Mojtaba Seyedhosseini, and Yonghui Wu. Coca: Contrastive captioners are image-text foundation models. *arXiv preprint arXiv:2205.01917*, 2022.
- [57] Licheng Yu, Patrick Poirson, Shan Yang, Alexander C Berg, and Tamara L Berg. Modeling context in referring expressions. In *ECCV*, pages 69–85, 2016.
- [58] Licheng Yu, Hao Tan, Mohit Bansal, and Tamara L Berg. A joint speaker-listener-reinforcer model for referring expressions. In *IEEE CVPR*, pages 7282–7290, 2017.
- [59] Yuqian Yuan, Wentong Li, Jian Liu, Dongqi Tang, Xinjie Luo, Chi Qin, Lei Zhang, and Jianke Zhu. Osprey: Pixel understanding with visual instruction tuning. *IEEE CVPR*, 2024.
- [60] Yu Yun, Sen Wang, Mingzhen Hou, and Quanxue Gao. Attributes learning network for generalized zero-shot learning. *Neural Networks*, 150:112–118, 2022.
- [61] Yan Zeng, Xinsong Zhang, and Hang Li. Multi-grained vision language pre-training: Aligning texts with visual concepts. In Kamalika Chaudhuri, Stefanie Jegelka, Le Song, Csaba Szepesvári, Gang Niu, and Sivan Sabato, editors, *ICML*, volume 162, pages 25994–26009, 2022.
- [62] Xiaohua Zhai, Basil Mustafa, Alexander Kolesnikov, and Lucas Beyer. Sigmoid loss for language image pre-training. In *IEEE ICCV*, pages 11975–11986, 2023.
- [63] Sanyi Zhang, Zhanjie Song, Xiaochun Cao, Hua Zhang, and Jie Zhou. Task-aware attention model for clothing attribute prediction. *IEEE TCSVT*, 30(4):1051–1064, 2019.
- [64] Shilong Zhang, Peize Sun, Shoufa Chen, Min Xiao, Wenqi Shao, Wenwei Zhang, Kai Chen, and Ping Luo. Gpt4roi: Instruction tuning large language model on region-of-interest. *arXiv preprint arXiv:2307.03601*, 2023.
- [65] Susan Zhang, Stephen Roller, Naman Goyal, Mikel Artetxe, Moya Chen, Shuohui Chen, Christopher Dewan, Mona T. Diab, Xian Li, Xi Victoria Lin, Todor Mihaylov, Myle Ott, Sam Shleifer, Kurt Shuster, Daniel Simig, Punit Singh Koura, Anjali Sridhar, Tianlu Wang, and Luke Zettlemoyer. OPT: open pre-trained transformer language models. *arXiv preprint arXiv:2205.01068*, 2022.
- [66] Youcai Zhang, Xinyu Huang, Jinyu Ma, Zhaoyang Li, Zhaochuan Luo, Yanchun Xie, Yuzhuo Qin, Tong Luo, Yaqian Li, Shilong Liu, et al. Recognize anything: A strong image tagging model. *arXiv preprint arXiv:2306.03514*, 2023.
- [67] Yuzhong Zhao, Qixiang Ye, Weijia Wu, Chunhua Shen, and Fang Wan. Generative prompt model for weakly supervised object localization. In *Proceedings of the IEEE/CVF International Conference on Computer Vision*, pages 6351–6361, 2023.

- [68] Yuzhong Zhao, Yue Liu, Zonghao Guo, Weijia Wu, Chen Gong, Fang Wan, and Qixiang Ye. Controlcap: Controllable region-level captioning, 2024.
- [69] Yiwu Zhong, Jianwei Yang, Pengchuan Zhang, Chunyuan Li, Noel Codella, Liunian Harold Li, Luowei Zhou, Xiyang Dai, Lu Yuan, Yin Li, et al. Regionclip: Region-based language-image pretraining. In *IEEE CVPR*, pages 16793–16803, 2022.

## A Comprehensive Related Works

**Vision-Language Models.** These methods aim to learn multi-modality comprehension ability given image-text pairs. Benefit from powerful foundation models [48, 13, 12, 65, 9] and huge amount of vision-language data corpus [43], VLMs have achieved unprecedented performance across vision-language tasks such as image-text retrieval [28, 29, 50, 31], visual question answering (VQA) [28, 29, 11, 33], image captioning [28, 29, 11, 33], image generation [42, 67], and few-shot learning [1, 56].

According to the training objectives, VLMs can be categorized to three: (i) Image-text contrastive learning [39, 69, 56, 50], (ii) Image-text matching [27, 28, 29, 2], and (iii) Language modeling [56, 33, 28, 29, 1, 37, 59, 40, 49]. To accomplish region-level tasks, some of these models [37, 59, 40, 4, 69, 49] are trained on region-text pairs to unlock their region-level comprehension ability. However, for a given region, existing models [24, 51, 64, 59, 4, 69] attempt to learn one representation to fit all tasks, which makes it hard to balance the context or detail demand for region-level tasks. To conquer this issue, DynRefer formats the region representation as a manifold of stochastic multi-view, which can dynamically adjust the representation for tasks by switching views.

**Region-level Multi-modality Tasks.** These predict region-level semantics (*e.g.*, classes, attributes, captions) for given (referred) image regions. The predictions of region-level semantics are crucial for many vision-language tasks such as region recognition, attribute detection, and region-level captioning.

(i) *Region recognition.* The most typical methods are from the object detection domain [16, 19], which trains a classifier and a regressor for a close set of semantics. With the rapid development of VLMs, classifying regions in an open set has become a common practice. The methods based on contrastive learning [69, 35, 39] get the class by calculating the similarity between region embeddings and text embeddings. While the methods based on language modeling [17, 33, 7, 5, 64] query the large language model (LLM) to select the most likely class of given regions among an open set. This research trend urge the development of resolution adaptability, which is crucial to improve the classification accuracy by dynamically using the context information.

(ii) *Attribute detection.* Given image regions, this predicts structured and fine-grained information, such as color, texture, shape, and material. Early studies focused on specific domains such as object parts [15], clothes [63], faces [20], and animals [52], which limits their potential. With the release of large-scale attribute datasets including COCO Attributes [36], Visual Genome [25], and VAW [38], recent studies [38, 60] realized attribute detection by training multi-class classification networks. Inspired by CLIP [39], OVAD [4], OvarNet [8] learn to predict attributes from captions, which rely less on densely annotated attributes and can make predictions in an open vocabulary manner.

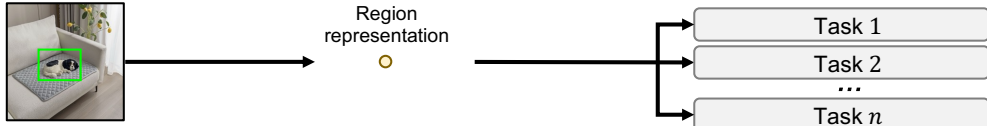
(iii) *Region-level captioning.* With the rapid development of VLMs, the generation of region-level captions based on large multimodal models (LMMs) has become a widespread practice. Shikra [7], GPT4RoI [64], Kosmos-2 [37], ASM [49], MiniGPT-v2 [6], RegionGPT [17], Alpha-CLIP [47], GLaMM [40], and Osprey [59] have equipped LMMs with region-level comprehension ability. They have achieved the state-of-the-arts on region-level captioning [7, 37, 40, 59, 47]. Dense captioning is a task closely associated with region-level captioning. Its objective is to identify and produce detailed descriptions for densely populated object regions within an image [24, 30, 44, 51, 35]. As a pioneered method, FCLN [24] used a localization network to locate regions and a recurrent network to generate captions. With the observation that visual concepts in an image are associated with each other, JIVC [54], COCG [30], and CAG-Net [55] model the relationship between visual concepts in the image and improves the quality of captions. With the advancement of transformer [48], there has been a significant improvement in scene captioning [44, 51, 35]. GRiT [51] unifies the training of classification and captioning by treating object categories as brief captions. CapDet [35] further combines dense captioning with open-world detection in a pretraining setup.

The trend of exploiting region-level information for fine-grained vision-language tasks urges the development of resolution adaptability, which is crucial to improve the accuracy of recognition, attribute detection, and dense captioning by dynamically using the context information. Furthermore, for the multiple types of referring tasks, existing methods ignore the inherent similarity between region-level multi-modality tasks. There is an urgent requirement to unify these tasks from the perspective of model training. Such unification is expected to bring mutual improvement among tasks so that state-of-the-art results can be achieved for all tasks with a single model.

**Dynamic Resolution of Visual Cognition.** The research in the visual cognition area has shown that the human vision system has the capability of dynamic resolution. The fovea, situated in the central part of the retina, possesses the highest resolution view, while other parts of the retina dynamically perceive context views for details [10]. Recent research [3] has demonstrated that foveal and peripheral vision are closely linked and differences in appearance between peripheral and foveal vision can be adjusted through re-calibration [46]. In contrast, computer vision systems lack such a dynamic mechanism and instead capture only a static view [18]. To simulate the dynamic resolution mechanism through computer vision is non-trivial.

## B Explanation: A Manifold Perspective

### Conventional region-level multi-modality methods



### DynRefer (Ours)

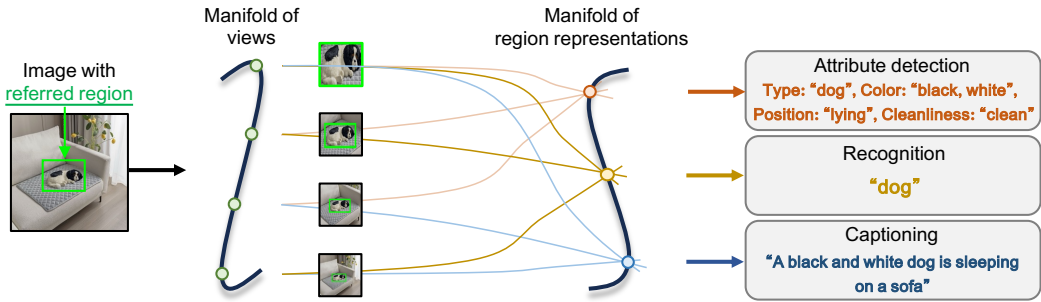


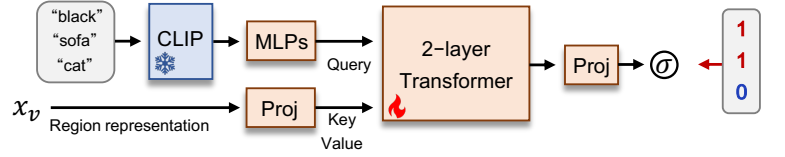
Figure 7: Comparison of the conventional region-level multi-modality methods(upper) with DynRefer approach(lower) in a manifold perspective. Conventional methods statically encode an image to a region representation, which is used to handle multi-tasks. DynRefer learns a manifold of region representation, on which weaker yet more dense representations can be sampled for diverse multi-modality tasks.

Conventional resolution-fixed methods [37, 59, 17] learn a single region representation for a given image region, which is used to solve diverse multi-modality tasks, Fig. 7(upper). Due to the diversity of tasks, the region representation has to be strong enough to achieve good performance for all tasks, which results in high-resolution input demand and large computational cost. Instead of learning a single strong region representation, DynRefer aims to learn region representation as a manifold, from which weaker yet more dense representations can be sampled for tasks, thus achieving good performance on all tasks, Fig. 7(lower). DynRefer first build a manifold of nested views by cropping and resizing the original image. The views on the manifold are low-resolution and can be encoded efficiently. They focus on different characteristics of the region, *i.e.*, region details and image context. Then, another manifold, *i.e.*, manifold of region representation is built based on the previous manifold. It samples random views and fuse them into a region representation. On the manifold region representation, specialized region representations can be sampled for diverse multi-modality tasks, which enhances the performance for all tasks.

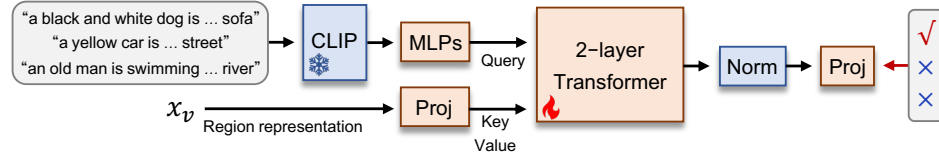
## C Detailed Model Settings

**Structure of the Decoder for Region Tagging.** The structure of the decoder ( $D_{tag}$ ) is shown in Fig. 8(top). The region representation  $x_v$  is first mapped to a low-dimension embedding with a linear

### $D_{tag}$ : Region tagging



### $D_{rtc}$ : Region-text contrastive learning



### $D_{llm}$ : Language modeling

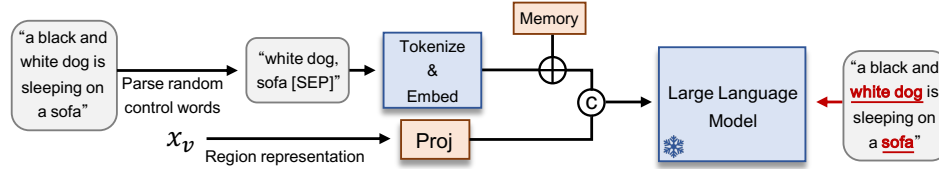


Figure 8: The detailed structure of multi-modality task decoders  $D_*$  of DynRefer. “Proj” is a linear projection layer. “ $\sigma$ ” is the sigmoid activation function. “Memory” is a learnable embedding. The “2-layer transformer” denotes query-based decoders [34, 66] that contains only cross-attention layers and feed forward networks.

projection layer. Meanwhile, predefined tags are encoded by a frozen CLIP [23] and multi-layer perceptrons. Then, a query-based decoder [34, 66] (“2-layer Transformer” in Fig. 8) is used to calculate the confidences of the tags. The confidences are optimized by asymmetric loss [41].

**Structure of the Decoder for Region-text Contrastive Learning.** The structure of the decoder ( $D_{rtc}$ ) is shown in Fig. 8 (middle). It has a similar structure with  $D_{tag}$ .  $D_{rtc}$  normalizes the outputs from the query-based decoder and project them into similarity scores, which are optimized by SigLIP loss [62].

**Structure of the Decoder for Language Modeling.** The structure of the decoder ( $D_{llm}$ ) is shown in Fig. 8(down). Following ControlCap [68], we introduce control words to alleviate the caption degeneration issue, which refers to that pre-trained multi-modality models tend to predict the most frequent captions but miss the less frequent ones. During training, the control words are parsed from the ground-truth captions and are randomly dropped in accordance with a Bernoulli distribution. The remained control words are shuffled and combined with a [SEP] token to form a control sentence, *i.e.*, “white dog, sofa [SEP]” in Fig. 8. The sentence is encoded into the control embedding by the tokenizer and word embedding layer of the large language model. After that, a learnable memory unit is added to the control embedding. Finally, the control embedding and the projected region representation are concatenated and jointly sent into the large language model for text generation.

**Inference with Trained Decoders.** With trained decoders, the region representation  $x_v$  can be decoded into region-level language descriptions, including tags, classes, attributes and captions. Their production are elaborated below:

(i) *tags*. The tags of the region are generated by  $D_{tag}$ . Following [22, 66], we use a set of 4585 tags. During inference, we first query the decoder with the predefined tags to get the confidences. Then, the tags are filtered by a tagging threshold.

(ii) *classes*. The class of the region is generated by  $D_{rtc}$ . During inference, we query the decoder with the template “a photo of a {cls}” and select the class with the highest score.

Table 6: Effectiveness of keeping the view containing only the referred region ( $t_1 = 0$ ) sampled in DynRefer on region-level multi-modality benchmarks.

	$t_1 = 0$	OVAD mAP (%)	COCO Acc (%)	VG-COCO mAP (%)	RefCOCOg	
					CIDEr	METEOR
1	✗	23.0	74.0	44.4	110.0	17.2
2	✓	<b>28.7</b>	<b>90.3</b>	<b>47.4</b>	<b>118.6</b>	<b>18.2</b>

Table 7: Effectiveness of the nested views in multi-view construction in DynRefer on region-level multi-modality benchmarks.

	Nested views	OVAD mAP (%)	COCO Acc (%)	VG-COCO mAP (%)	RefCOCOg	
					CIDEr	METEOR
1	✗	25.5	83.7	43.3	114.0	17.5
2	✓	<b>28.7</b>	<b>90.3</b>	<b>47.4</b>	<b>118.6</b>	<b>18.2</b>

(iii) *attributes*. The attributes of the region are generated by  $D_{rtc}$ . During inference, we first query the decoder with attribute templates following OVAD [4], *e.g.*, “the object has {attr}”. Then, attributes with high scores are selected as the results.

(iv) *captions*. The caption of the region is generated by  $D_{llm}$ . During inference, we first use the tags of high confidence to form a control sentence, *i.e.*, “{tag1}, {tag2}, {tag3}, …, [SEP]”. Then, the control sentence and the region representation are used to control the language model for caption generation.

## D Additional Experimental Results

**Multi-view Construction: Sampling the View Containing Only the Referred Region.** Tab. 6 compares the results that the view containing only the referred region keeps sampled (“✓”) or is randomly sampled during training (“✗”). It can be seen that the view containing only the referred region is crucial for all multi-modality tasks. It should always be sampled to maintain good performance, *i.e.*, keeping the interpolation coefficient of the first view  $t_1$  to 0.

**Multi-view Construction: Nesting Views.** The effectiveness of nesting views in multi-view construction is shown in Tab. 7. For line 1, the views are selected by random cropping regions that cover the referred area from the original image. Compared to line 1, the proposed multi-view construction performs better for all tasks.

**Stochastic Multi-view Embedding: Align module.** The effectiveness of the align module is validated in Tab. 8. By spatially aligning the region embeddings of multiple views, the performance on all tasks are improved.

**Statistics of Parameters and FLOPS.** The parameter and flop composition of DynRefer is shown in Tab. 9. DynRefer has few trainable parameters and can be trained efficiently.

**Complete Performance Comparison with SOTA Methods.** Tab 10 11 12 13 show the complete performance comparison of the proposed DynRefer and the state-of-the-art (SOTA) methods (extension of Tab. 1 2 3 4 in the main document).

## E Detailed Experimental Settings

**Implementation Details.** DynRefer is implemented upon the LAVIS [26] framework, where large language model and vision resampler are respectively initialized by Flan-T5<sub>XL</sub> [9] and Q-former [29]. All the sampled views are resized to  $224 \times 224$  resolution. All models are trained using 8 NVIDIA A800 GPUs by 5 epochs, with the Adam optimizer where the batch size is set to 512. The total training time is less than 20 hours. The initial learning rate is set to  $1 \times 10^{-4}$  with a cosine learning rate decay.

Table 8: Evaluation of the align module of DynRefer on region-level multi-modality benchmarks. Line 2 corresponds to line 9 in Tab. 5 in the main paper.

	Align module	FLOPs	OVAD mAP (%)	COCO Acc (%)	VG-COCO mAP (%)	RefCOCOg	
						CIDEr	METEOR
1	$\times$	790G	27.3	88.4	47.1	113.6	17.9
2	$\checkmark$	792G	<b>27.3</b>	<b>88.9</b>	<b>47.3</b>	<b>117.7</b>	<b>18.2</b>

Table 9: Analysis of parameter composition of DynRefer. Modules that contain very few parameters are omitted for clarity.

	ViT	Align module	Vision Resampler	$D_{tag}$	$D_{rtc}$	CLIP	LLM
Trainable Parameters (%)	$\times$	$\checkmark$	$\checkmark$	$\checkmark$	$\checkmark$	$\times$	$\times$
Flops (G)	23.78	0.20	2.53	0.05	0.05	2.99	68.79
	783.5	2.1	6.4	6.2	0.4	6.5	80.1

**Datasets.** For all tasks, DynRefer is trained using Visual Genome (VG) [25] and RefCOCOg [57]. For ablation studies, DynRefer is trained using VG-COCO [44] and RefCOCOg [57]. For evaluation, we evaluate the region-level captioning performance on VG, VG-COCO [44], and RefCOCOg, the open vocabulary attribute detection performance on OVAD [4], and the region recognition performance on COCO [32].

**Evaluation Metrics.** For region-level captioning, the METEOR score and CIDEr score are adopted as the evaluation metrics following [40, 59, 17]. For dense captioning, mean Average Precision (mAP) [24] is adopted as the evaluation metric following [24, 35]. The mAP is calculated across a range of thresholds for both localization and language accuracy, *i.e.*, the intersection over union (IoU) thresholds (0.3, 0.4, 0.5, 0.6, 0.7) are used for localization and the METEOR score’ thresholds (0, 0.05, 0.1, 0.15, 0.2, 0.25) is adopted for evaluating the language generation. Since DynRefer lacks the capability to perform object detection, we utilize a GRiT [51] model trained on VG to acquire object locations. For open vocabulary attribute detection, mAP is adopted as the evaluation metric following OVAD [4]. For region recognition, mAP and Accuracy (Acc.) are are adopted as the evaluation metrics following [17, 69].

**Combining with Existing Detectors.** Considering that dense captioning requires the model to initially generate dense bounding-boxes, we utilize a GRiT [51] model trained on the VG to acquire object locations. During the inference stage, we use the bounding boxes and object scores predicted by GRiT, and then replace its predicted caption with DynRefer to get the final result.

**Setting of Optimization.** The detailed hyperparameters during training and inference are shown in Tab. 14.

## F Additional Visualization Results

We provide additional visualization results of Fig. 6 in the main document. The results are shown in Fig. 9 10.

## G Limitations

Though DynRefer significantly outperforms previous state-of-the-arts on multiple multi-modality tasks, it still doesn’t perfectly mimic the visual cognition system of human. A real human can adjust the resolution of visual inputs in a more dynamic and flexible way. Better simulation strategy can be explored in the future work.

Table 10: Region-level captioning performance of the proposed approach and the state-of-the-art methods on RefCOCOg and VG datasets.

Method	Model size	RefCOCOg		VG	
		METEOR	CIDEr	METEOR	CIDEr
SLR+Rerank <sub>CVPR'17</sub> [58]	<1B	15.9	66.2	-	-
GRiT <sub>ARXIV'22</sub> [51]	<1B	15.2	71.6	17.1	142.0
Kosmos-2 <sub>ICLR'24</sub> [37]	1.6B	14.1	62.3	-	-
GPT4RoI <sub>ARXIV'23</sub> [64]	7B	-	-	17.4	145.2
RegionGPT <sub>CVPR'24</sub> [40]	7B	16.9	109.9	17.0	145.6
GLaMM <sub>CVPR'24</sub> [40]	7B	16.2	105.0	18.6	157.8
Alpha-CLIP+LLaVA <sub>CVPR'24</sub> [47]	7B	16.7	109.2	18.9	160.3
Osprey <sub>CVPR'24</sub> [59]	7B	16.6	108.3	-	-
DynRefer (Ours)	4.2B	<b>18.1</b>	<b>115.7</b>	<b>21.2</b>	<b>190.9</b>

Table 11: Dense captioning performance of the proposed approach and the state-of-the-art methods on VG and VG-COCO datasets.

Methods	GT localization	mAP(%)		
		VG V1.0	VG V1.2	VG-COCO
FCLN <sub>CVPR'16</sub> [24]	✗	5.4	5.2	-
JIVC <sub>CVPR'17</sub> [54]	✗	9.3	10.0	-
ImgG <sub>AAAI'19</sub> [30]	✗	9.3	9.7	-
COCD <sub>AAAI'19</sub> [30]	✗	9.4	9.8	7.9
COCG <sub>AAAI'19</sub> [30]	✗	9.8	10.4	8.9
CAG-Net <sub>CVPR'19</sub> [55]	✗	10.5	-	-
TDC <sub>TNNLS'22</sub> [44]	✗	11.5	11.9	11.9
GRiT <sub>ARXIV'22</sub> [51]	✗	15.5	16.4	-
CapDet <sub>CVPR'23</sub> [35]	✗	-	15.4	14.0
DCMSTRD <sub>TMM'24</sub> [45]	✗	13.6	13.4	16.1
DynRefer (Ours)	✗	<b>19.1</b>	<b>19.5</b>	<b>19.4</b>
FCLN <sub>CVPR'16</sub> [24]	✓	27.0	-	-
JIVC <sub>CVPR'17</sub> [54]	✓	33.6	-	-
CAG-Net <sub>CVPR'19</sub> [55]	✓	36.3	-	-
GRiT <sub>ARXIV'22</sub> [51]	✓	40.0	40.3	-
BLIP2 <sub>ICML'23</sub> [29]	✓	37.7	37.9	36.9
DynRefer (Ours)	✓	<b>47.2</b>	<b>47.4</b>	<b>47.6</b>

Table 12: Open vocabulary attribute detection performance of the proposed approach and the state-of-the-art methods on the OVAD dataset with the box-oracle setup (OVAD-Box).

Method	Backbone	OVAD-Box			
		All	Head	Medium	Tail
Chance [4]	-	8.6	36.0	7.3	0.6
CLIP <sub>ICML'21</sub> [39]	ResNet50	15.8	42.5	17.5	4.2
CLIP <sub>ICML'21</sub> [39]	ViT-B16	16.6	43.9	18.6	4.4
Open CLIP <sub>ICML'21</sub> [23]	ResNet50	11.8	41.0	11.7	1.4
Open CLIP <sub>ICML'21</sub> [23]	ViT-B16	16.0	45.4	17.4	3.8
Open CLIP <sub>ICML'21</sub> [23]	ViT-B32	17.0	44.3	18.4	5.5
ALBEF <sub>NeurIPS'21</sub> [27]	ViT-B16	21.0	44.2	23.9	9.4
X-VLM <sub>ICML'22</sub> [61]	Swin-B	28.1	49.7	34.2	12.9
OVAD-Baseline-Box <sub>CVPR'23</sub> [4]	ViT-B32	21.4	48.0	26.9	5.2
BLIP <sub>ICML'22</sub> [28]	EVA	24.3	<b>51.0</b>	28.5	9.7
BLIP2 <sub>ICML'23</sub> [29]	EVA	25.5	49.8	30.5	10.8
DynRefer (Ours)	ViT-L	28.2	50.9	34.5	12.5
DynRefer (Ours)	EVA	<b>29.2</b>	49.9	<b>35.7</b>	<b>14.0</b>

Table 13: Open vocabulary region recognition performance of the proposed approach and state-of-the-art methods on the COCO-2017 val set. Following RegionGPT [17] and RegionCLIP [69], we report the results of object classification given ground-truth boxes.

Method	Backbone	LLM	mAP	Acc. (%)
CLIP <sub>ICML'21</sub> [39]	ViT-L	-	58.9	-
RegionCLIP <sub>CVPR'22</sub> [69]	R50	-	58.3	-
LLaVA <sub>NeurIPS'23</sub> [33]	ViT-L	Vicuna-7B	-	40.0
Shikra <sub>ARXIV'23</sub> [7]	ViT-L	Vicuna-7B	-	53.9
GPT4RoI <sub>ARXIV'23</sub> [64]	ViT-L	LLaVA-7B	-	64.0
PVIT <sub>ARXIV'23</sub> [5]	ViT-L+R50	LLaVA-7B	-	64.5
ASM <sub>ICLR'24</sub> [49]	ViT-L	Hasky-7B	69.3	-
RegionGPT <sub>CVPR'24</sub> [17]	ViT-L	Vicuna-7B	70.0	80.6
DynRefer (Ours)	ViT-L	FlanT5 <sub>XL</sub> -3.4B	85.0	89.4
DynRefer (Ours)	EVA	FlanT5 <sub>XL</sub> -3.4B	<b>89.2</b>	<b>91.8</b>

Table 14: Detailed hyperparameters during training and inference.

Training	Value
GPUs	8× A800
batch size	512
training epochs	5
learning policy	cosine annealing
initial learning rate	1e-4
minimum learning rate	0
weight decay ratio	0.05
warmup steps	5000
Inference	Value
number of beams	5

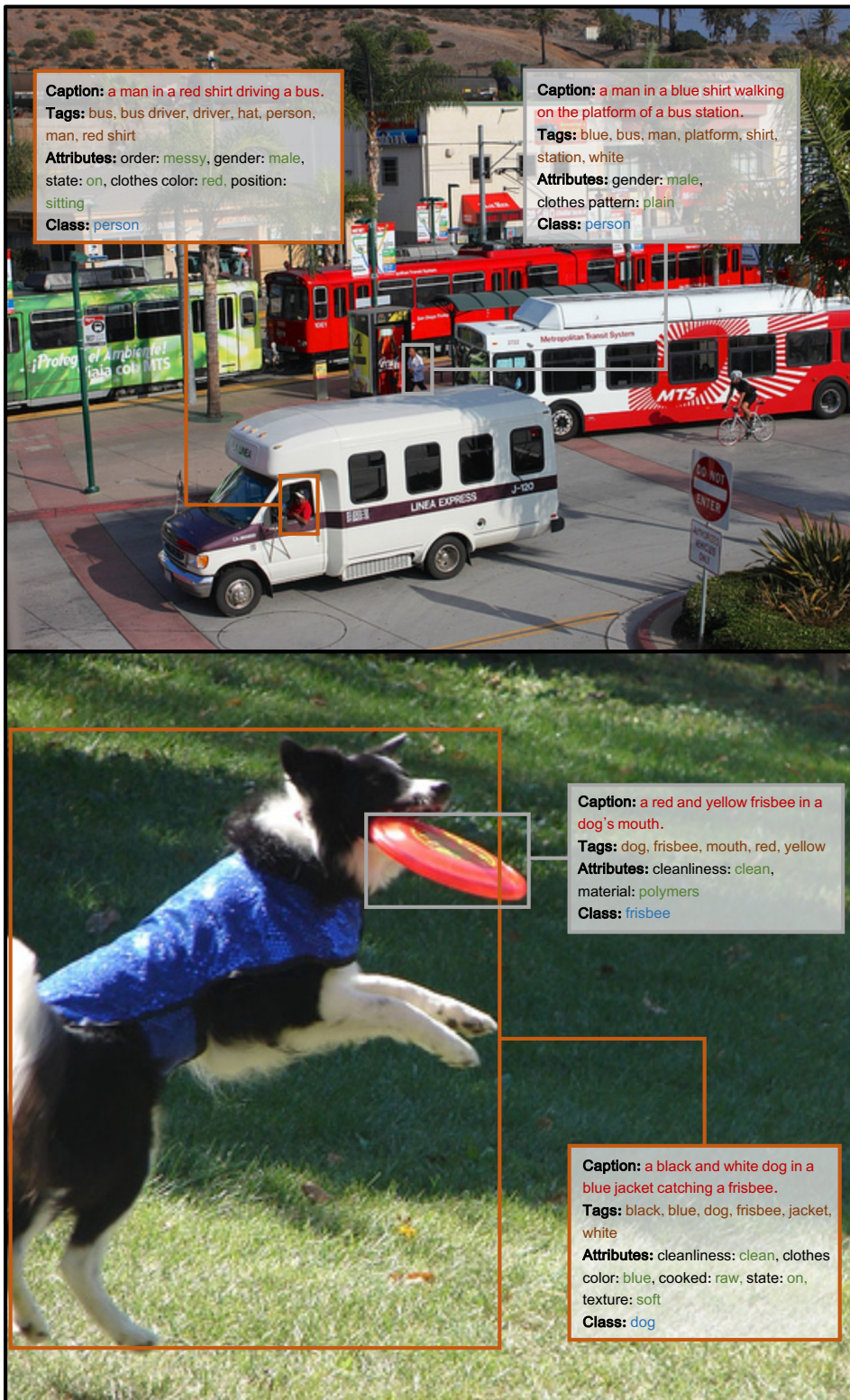


Figure 9: Illustration of DynRefer's multi-task capability. It can generate captions (red), tags (brown), attributes (green), classes (blue), using a single model, for multiple referred regions.

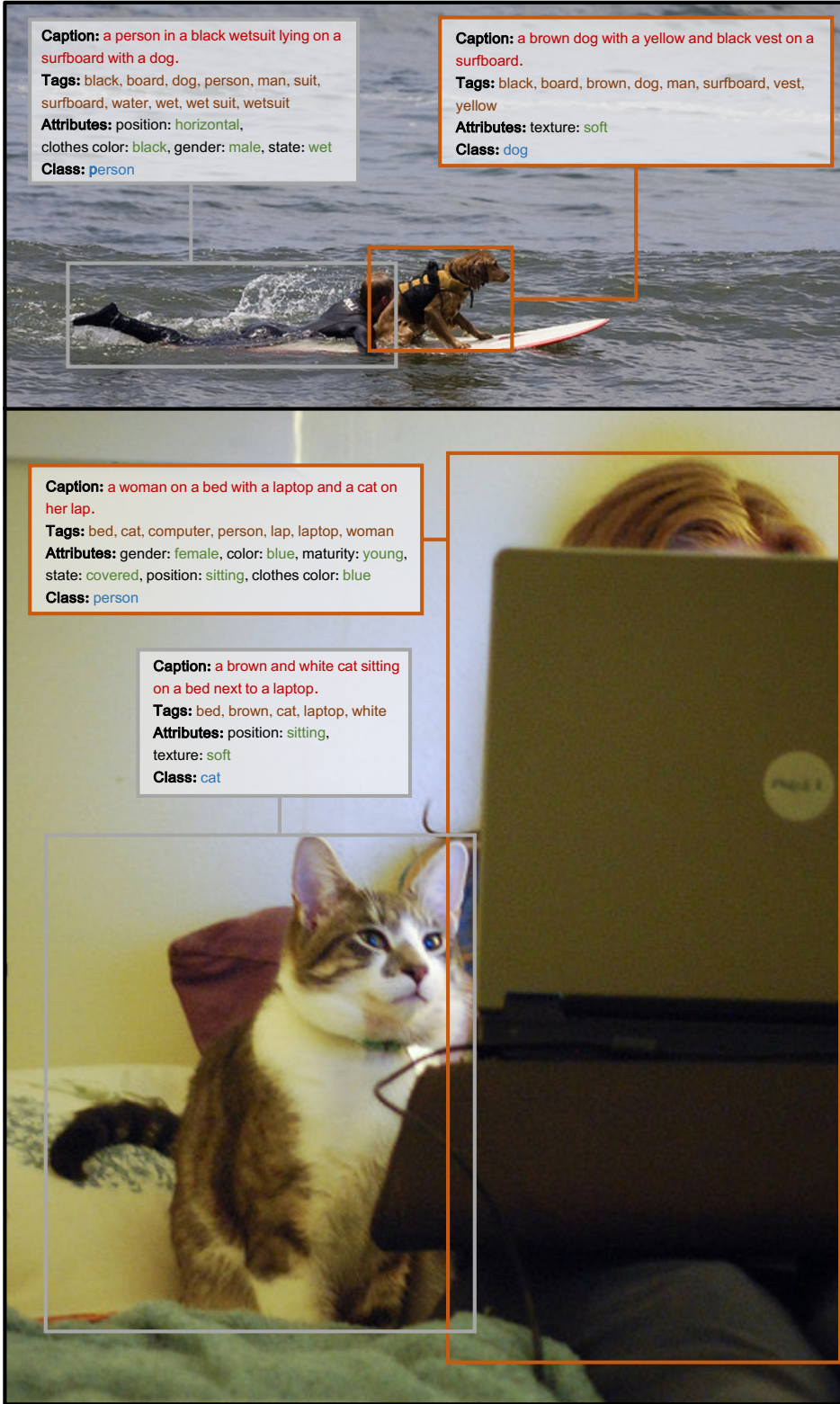


Figure 10: Illustration of DynRefer’s multi-task capability. It can generate captions (red), tags (brown), attributes (green), classes (blue), using a single model, for multiple referred regions.